• Basic Research •

Resveratrol mitigates hypoxia-induced mitochondrial oxidative damage and apoptosis *via* inhibition of TRPA1 channel in retinal pigment epithelial cells

Mehmet Argun[1], *Mustafa Nazıroğlu*[2,3,4]

[1]Departmant of Ophthalmology, School of Medicine, Suleyman Demirel University, Isparta 32260, Türkiye
[2]Neuroscience Research Center (NOROBAM), Suleyman Demirel University, Isparta 32260, Türkiye
[3]BSN Health, Analyses, Innovation, Consultancy, Organization, Agriculture, Industry LTD, Isparta 32260, Türkiye
[4]Department of Biophysics, School of Medicine, Suleyman Demirel University, Isparta 32260, Türkiye
Correspondence to: Mustafa Nazıroğlu. Department of Biophysics, School of Medicine, Suleyman Demirel University, Isparta 32260, Türkiye. mustafanaziroglu@sdu.edu.tr
Received: 2025-10-04 Accepted: 2026-01-28

Abstract

● **AIM:** To investigate the modulator action of resveratrol (RSV) through the suppression of transient receptor potential ankyrin 1 (TRPA1) on the hypoxia (HPO)-caused oxidative degeneration and apoptosis in human retinal pigment epithelial cells (ARPE19).

● **METHODS:** The control (CNT), RSV (50 μmol/L for 24h), HPO (200 μmol/L $CoCl_2$ for 24h), and HPO+RSV groups were induced in the ARPE19. Apoptosis, caspases (caspases 3, 8, and 9), oxidants [lipid peroxidation, oxygen free radical (OFR), and dysfunction of mitochondrial membrane], antioxidants (glutathione and glutathione peroxidase), Ca^{2+}, Zn^{2+} levels, live cell number and percentage were all measured in the cells of four groups.

● **RESULTS:** The HPO increased Ca^{2+} and Zn^{2+} fluorescence intensity in the cells. It also upregulated the apoptosis, caspases, and oxidant indicators while downregulating the antioxidants, and the count of live cells. TRPA1 agonist (cinnamonaldehyde) further upregulated these indicators (all P<0.05). When the HPO-induced increase in TRPA1 activation was treated with RSV and the TRPA1 antagonist (AP18), cell viability and antioxidants rose while the oxidant and apoptotic indicators decreased due to TRPA1 suppression (P<0.05).

● **CONCLUSION:** HPO exposure through TRPA1-mediated Ca^{2+} signaling, induces mitochondrial oxidative cell cytotoxicity and death, which may offer a treatment option for HPO-induced retinal disorders linked to increased OFR and Ca^{2+} influx.

● **KEYWORDS:** hypoxia; oxidative cytotoxicity; resveratrol; retinal pigment epithelial cells; TRPA1 channel
DOI:10.18240/ijo.2026.09.03

Citation: Argun M, Nazıroğlu M. Resveratrol mitigates hypoxia-induced mitochondrial oxidative damage and apoptosis *via* inhibition of TRPA1 channel in retinal pigment epithelial cells. *Int J Ophthalmol* 2026;19(9):1676-1686

INTRODUCTION

Retinal hypoxia (HPO) plays a major role in the development of dysfunctional neovascularization[1]. In neovascular retinal diseases such as retinal vein occlusion, diabetic retinopathy, age-related macular degeneration, and retinopathy of prematurity, it is therefore the primary cause of visual loss[1-2]. Inadequate management of this condition could lead to blindness. The usefulness of growth factors of anti-vascular endothelial medications in the modulation of neovascular retinal diseases has been demonstrated in recent years[1-2]. However, even after receiving several injections, some patients continue to experience drug resistance or insufficient responses due to the abnormal production of cytosolic oxygen free radicals (cOFR) and mitochondrial oxygen free radicals (mOFR) in retinal cells[2-3]. Investigating and developing novel anti-angiogenic therapies is therefore imperative.

The substitution of cobalt chloride ($CoCl_2$) for ferrous ions in heme can harm heme proteins and DNA and impair their capacity to sense oxygen[4]. $CoCl_2$ has been widely used as a retinal HPO induction in recent studies[5-6]. It also increases the generation of cOFR and mOFR in cells, which exacerbates retinal death and apoptosis[7]. The generation of mOFR and cOFR-caused overload Ca^{2+} influx through the stimulation of transient receptor potential (TRP) vanilloid 4 (TRPV4) and TRP melastatin 2 (TRPM2), is strongly associated with apoptosis and oxidative damage in the retina, heart,

and neurons caused by $CoCl_2$[7-10]. HPO-induced increases through TRP channel stimulation in intracellular free Ca^{2+} ($[Ca^{2+}]_i$) and zinc ($[Zn^{2+}]_i$) concentrations can target mitochondrial accumulation, which in turn causes mOFR and intracellular oxygen free radicals (iOFR), cell degeneration, and apoptosis in the cells of human retinal pigment epithelial cell 19 (ARPE19) and neurons[7-8]. Furthermore, $CoCl_2$-caused dysfunction of mitochondrial membrane potential (miMDys) has been shown to stimulate caspase 3 (CASP/3), caspase 8 (CASP/8), and caspase 9 (CASP/9) in ARPE19 cells for inducing apoptosis[7,11-12].

TRP ankyrin 1 (TRPA1) is a member of TRP. TRPA1 is stimulated by cinnamaldehyde (CNM)[13], while AP18 is an antagonist of TRPA1[14]. There are cysteine-free sulfhydryl groups in the cytoplasmic N terminus of TRPA1, and they are the main targets for the OFRs[15]. Hence, TRPA1 in a number of cells, including retinal cells, has a strong sensitivity to the mOFR and cOFR[16]. In animal models of HPO, the capacity of mOFR and cOFR byproducts to gate TRPA1 has been found to be a key mechanism of damage to the kidneys, heart, and neurons[4,17-18]. HPO-mediated TRPA1 activation caused glioblastoma apoptosis through the stimulation of caspases, although its suppression by AP18 reduced the apoptosis through the inhibition of caspases[19]. The role of TRPA1 in HPO-mediated apoptosis, cOFR, and mOFR remains unclear.

Plant-derived products contain natural antioxidants, which are major sources of many current therapies. The biological impacts of natural plant-derived compounds on human health are therefore of enormous practical importance[20-21]. For many years, hypoxic disorders have been treated using antioxidants derived from plants[22]. Antioxidants generated from plants are therefore particularly interesting because of their enormous potential for treating hypoxic human diseases[21-22]. Resveratrol (RSV) has become one of the most promising plant-derived antioxidants for combating oxidative cytotoxicity and HPO-induced cell death in eye disorders[21]. RSV has been detected in several fruits and plants, although it is particularly found in grapes[21-22]. There is growing evidence that RSV may have protective roles in pathological conditions such as oxidative stress and apoptosis[23-25]. Indeed, RSV inhibited the TRPM2 channel in several cells except ARPE19, which in turn controlled the increases in mOFR, apoptosis, and Ca^{2+} influx induced by diabetes mellitus[24-26]. Additionally, by inhibiting TRPM2 in SH-SY5Y neural cells, RSV regulated HPO-induced oxidative damage and death[27]. The involvement of RSV as a TRPA1 inhibitor in rat neurons was reported[27]. Therefore, by inhibiting the TRPA1 channel, RSV treatment of ARPE19 cells may modify HPO-induced Ca^{2+} entry, apoptosis, and mitochondrial oxidative degeneration.

The action of RSV and TRPA1 on mitochondrial oxidative degeneration and apoptosis in HPO-mediated ARPE19 cells is currently unknown. In this study, we first investigated the action of TRPA1 in the hypoxic injury in ARPE19 by measuring their levels of apoptosis and mitochondrial oxidative stress. Second, the protective effect of RSV on oxidative degeneration and apoptosis was investigated by inhibiting TRPA1. Our results indicate that RSV incubation diminishes the amount of cell death and mitochondrial oxidative degeneration by inhibiting TRPA1 in ARPE19.

MATERIALS AND METHODS

Cell Culture The ARPE19 cells were provided by Glasgow Caledonian University, UK (Dr. Xinhua Shu). According to a previous study[28], the TRPA1 channel in the ARPE19 exists naturally. Therefore, we used ARPE19 cells for the TRPA1 investigation. A combination of Ham's F-12/Dulbecco's Modified Eagle's media (DMEM; low glucose-1 g/L) with L-glutamine, fetal bovine serum (10%), and antibiotic combination (penicillin/streptomycin and 1%; Diagvonum, Ebsdorfergrund, Germany) was used to cultivate the ARPE19[7]. In an NB-203QS (Gyeonggi-do, South Korea) cell culture incubator, the cells of ARPE19 were grown in 25 cm^2 flasks with a humidity level of 60%–80% and a 5% CO_2/95% air ratio.

Study Groups Four main groups (each with $\times 10^6$ cells) were induced in the cells as control (CNT), RSV, HPO, and HPO+RSV. The cells in the CNT group were kept in the cell culture incubator (NB-203QS**)** for a full day without RSV and $CoCl_2$ incubations. Cells in the RSV group were cultured with 50 μmol/L RSV for 24h[29-30]. The antioxidant and ARPE19 protective roles of 50 μmol/L RSV after 24h incubation were reported[29-30]. For induction of HPO, 200 μmol/L $CoCl_2$ (24h) incubation was used in the ARPE19 cells[4,31]. Therefore, the RSV and $CoCl_2$ dosages in the HPO and RSV groups were utilized in this investigation. The cells in the HPO+RSV group were cultured for 24h with 200 μmol/L $CoCl_2$ and 50 μmol/L RSV. It was reported that AP18 (20 μmol/L 30min) is a non-specific inhibitor of TRPA1[14,32-33]. In certain investigations, we established a fifth group and supplied the ARPE19 cells in that group an additional half-hour of exposure to 20 μmol/L AP18[19,32-33].

The CASY cell counter and plate reader experiments used cells from 25 cm^2 flasks. However, we used attached cells in the 35-mm dishes with glass bottoms (Corporation of Mattek, Ashland, MA, USA) for the imaging records. In the studies, the cells were stimulated by the TRPA1 agonist (0.1 mmol/L CNM), although they were inhibited by the TRPA1 antagonist (20 μmol/L AP18). The imaging analyses were performed on the cells in the dishes under LSM800 laser scan confocal microscope (LSCM/800) or fluorescent microscopy camera

(Axiocam 702; Carl Zeiss, Oberkochen, Germany). They were also attached to an objective (20×/0.8 Plan-Apochromat) and Axio Observer.Z1/7 microscope.

Stock solutions of fluorescent dyes, RSV, and AP18 were prepared in dimethyl sulfoxide. CNM stock solution was diluted in extracellular buffer with Ca^{2+}[32]. After that, the cell culture medium was used to dilute all of the compounds to the proper concentrations. Diluted CNM (0.1 mmol/L) and AP18 (20 μmol/L) were freshly added to the extracellular buffer for stimulation and inhibition of TRPA1, respectively.

Cell Viability, Number, and Debris Counts Live cell and debris (biological debris remaining when a cell dies) were counted using an automated CASY Model TT cell counter (Roche, Reutlingen, Germany)[26]. The CASYtone buffer, an electrolyte developed especially for cell viability percentage, number, and debris, is used to suspend the cells during the cell counter process. The cell viability is presented as percentage changes. Viable cell and debris numbers are shown as 1×10^6 cells per milliliter and 1×10^5 cells per milliliter, respectively.

Analyses of the Apoptosis and Caspases A commercial ApoPercentage (Cat # A1000) kit for the apoptosis test was bought from Biocolor Ltd. (Northern Ireland). For the caspase and apoptosis investigations, 1×10^4 cells were used in each well of 96-well plates. After a single 1× phosphate buffered saline (PBS) wash, the cells were suspended using the APOPercentage staining solution in each well of 96-well white plates. An Infinite PRO 200 microplate reader of Tecan GmbH (Groedig, Austria) was used to measure absorbance changes[34]. Previously published studies[34-35] provided information on the chemical composition and process specifics of the CASP/3, CASP/8, and CASP/9 analysis activities. Using the Infinite PRO 200, the cleavage of the substrates of CASP/3 (Ac-DEVD-AMC), CASP/8 (AC-IEPD-AMC), and CASP/9 (Ac-LEHD-AFC) substrates (Bachem, Heidelberg, Germany) was assessed. A black 96-well microplate was filled with 15 μL of the cell solution. The substrate cleavages were performed at wavelengths ranging from 360 nm for excitation to 460 nm for emission.

After these ApoPercentage and caspase substrate loadings, the cells of four groups (CNT, RSV, HPO, and HPO+RSV) underwent apoptosis and caspase assays. To measure the TRPA1-dependent apoptosis induction and caspase releases, apoptosis and caspase assays were performed on the cells in the four groups following TRPA1 activation (0.1 mmol/L CNM for 30min) and block (20 μmol/L AP18 for 30min). The percentage changes of CNT were used to show the outcomes of caspases and apoptosis.

Assays for the Percentage of Propidium Iodide-Positive Cells Propidium iodide (PI; 5 μg/mL; Cat # P1304MP) and Hoechst 33342 (4 μg/mL; Cat # H3570) were obtained from Thermo Fisher Scientific (Waltham, MA, USA), in order to visualize nuclei and quantify PI-positive (dead or damaged) cells. The images were captured with an LSCM/800 and a computer. Argon lasers were used to stimulate PI and Hoechst 33342 at 561 nm and 405 nm, respectively. The percentage of dead cells was calculated by dividing the number of PI-positive cells by the number of red nuclei[11].

cOFR and mOFR Measurements The fluorescent version [2',7'-dichlorofluorescein (DCF)] of 2,7-dichlorofluorescein diacetate (H_2DCFDA; Cat # D399) was used to monitor the generations of cOFR. The measurement of mOFR was performed using the MitoSOX Red reagent (Cat #: M36008). The cells in the 35-mm dishes were loaded with a mixture of 2 μmol/L H_2DCFDA and 2 μmol/L MitoSOX Red for 25min at 37°C in the dark according to the manufacturer's instructions (Thermo Fischer Scientific). The cells were recorded after being washed twice with 1×PBS, and Zeiss efficient navigation (ZEN) blue software was used to quickly identify any changes in fluorescence in the LSCM/800. The laser activation of DCF was kept at 488 nm in the LSCM/800, although MitoSOX activation was kept at 561 nm. The cOFR and mOFR readings were shown as a percentage of CNT after the fluorescence intensity was measured in arbitrary units.

Determining the Levels of miMDys The emission turns orange due to the accumulation of the cell membrane-permeant dye JC1 (Cat # T3168) in the damaged mitochondria (Thermo Fisher Scientific). MitoTracker Red (MitoTr; Cat #: M7513, Invitrogen, Eugene, Oregon, USA) is a fluorescent probe used to mark mitochondria. The cells in the dishes were treated with 1 μmol/L MitoTr and 2 μmol/L JC1 for 15–20min. Following dye washing, red (MitoTr), orange (JC1), bright field (BF; black/white), merge, and 2.5D photos were captured in the microscope (Axio Observer.Z1/7) using the fluorescent Axiocam 702 microscopy charge-coupled device (CCD) camera (Carl Zeiss). While the rate of the excitation/emission rate for JC1 was held at 593/595 nm, the rate of MitoTr was maintained at 578/598 nm. The miMDys findings were shown as a percentage of CNT.

Determining the Levels of Glutathione Fluorescence Intensity The cells were stained using a commercial ThiolTracker Violet probe (Cat #: T10095, Thermo Fisher Scientific) for 25 to 30min. For the glutathione (GSH) investigations, green images of the ARPE19 were taken using the LSCM/800. ThiolTracker Violet was continuously stimulated by an argon laser at 405 nm. The GSH findings were shown as a percentage of CNT.

Determining the Concentration of $[Zn^{2+}]_i$ Before green images of FlouZin3-AM in ARPE19 cells were captured using an LSCM/800 for the $[Zn^{2+}]_i$ concentration studies, the cells

were stained for 25 to 30min with a commercial FlouZin3-AM (Cat #: F24195) from Thermo Fisher Scientific. FlouZin3-AM was excited using an argon laser at 488 nm. The average $[Zn^{2+}]_i$ concentration was displayed using the fraction of CNT.

Measurement of the $[Ca^{2+}]_i$ Concentration Fluo-3 AM (1 μmol/L; Cat # F1241, Thermo Fisher Scientific) staining of the ARPE19 was performed for 60–90min at 37°C in the dark. After the dye was incubated, the cell culture media were extracted from the 35-mm dishes using 1× PBS washes, and then they were given extracellular buffer (0.5 mL) with Ca^{2+} (1.2 mmol/L). The CNM (0.1 mmol/L)-induced TRPA1 channel was reduced when AP18 (20 μmol/L) was given to the cells[19]. Using argon laser stimulation at 488 nm, the variations in green fluorescence intensity in the LSCM/800 were measured. The amount of $[Ca^{2+}]_i$ was displayed as a percentage of the control.

Glutathione Peroxidase, Lipid Peroxidation, and GSH Analysis A Shimadzu-UV1800 spectrophotometer (Kyoto, Japan) was used to determine the total protein content as well as the optic density (absorbance) values of lipid peroxidation (LPO; 532 nm)[36], GSH (412 nm)[37], and glutathione peroxidase (GPx; 412 nm)[38] in the ARPE19 samples. Micromoles per gram of protein were used to express the concentrations of GSH and LPO in ARPE19. GPx activity in the ARPE19 cells has been expressed as an IU per gram protein.

Statistical Evaluation To examine the existing data, SPSS statistical software program (Chicago, IL, USA) was utilized. Mean±standard deviation (SD) is displayed. A one-way analysis of variance (ANOVA) and Tukey's post hoc test were used to investigate the results. A *P*-value of less than 0.05 was considered statistically significant.

RESULTS

Values of Debris, Viable Cell Numbers, and Percentage The percentage of cell viability (Figure 1A) and number of viable cell (Figure 1B) were lower ($P<0.05$) in the HPO than in the CNT and RSV, whereas they were higher in the HPO+RSV than in the HPO only. The HPO group had higher debris numbers (Figure 1C; $P<0.05$), but the HPO+RSV groups had lower debris numbers compared to the HPO alone ($P<0.05$).

HPO Exposure Increased TRPA1 Activation, Causing to Increased Apoptosis, Caspases, and ARPE19 Cell Death ARPE19 cell death and apoptosis reduce the count of viable cells and increase the count of debris. By HPO-induced activation of CASP/3, CASP/8, and CASP/9 mediators, HPO treatment enhances apoptosis, but RSV treatment reduces the increases in apoptosis in neuronal cells[25-26]. The protective function of RSV against HPO-induced caspases and apoptosis, however, has not yet been studied. Thus, apoptosis (Figure 2A), CASP/3 (Figure 2B), CASP/8 (Figure 2C), and CASP/9 (Figure 2D) were investigated in this study. Using the LSCM/800, the red (PI), blue (Hoechst), merge, and 2.5D images were recorded (Figure 3A) for determining the percentages of PI-positive cell numbers (Figure 3B).

The HPO induced an increase in apoptosis and caspases (CASP/3, CASP/8, and CASP/9), as well as the count of PI-positive ARPE19 ($P<0.05$) in comparison to the RSV and CNT. After incubating with RSV and AP18, their levels were low in the HPO+CNM+AP18 and RSV+CNM+AP18. After CNM stimulation, they were higher in the HPO+CNM than in the HPO only ($P<0.05$). However, CNM does not increase the CASP/3, CASP/8, CASP/9, or apoptosis in the RSV and RSV+CNM. In the RSV or HPO+RSV groups, this had no effect on the CNM dependent increases in apoptosis, caspases, or the amount of PI-positive ARPE19.

HPO-Induced Generations of miMDys, mOFR, and cOFR It has been demonstrated that the accumulation of TRPA1-stimulated Ca^{2+} and Zn^{2+} in the mitochondria causes hyperpolarization, and that miMDys rises as mitochondrial depolarization falls[39-40]. Then, mOFR, LPO, and cOFR increase in response to an increase in miMDys[39-40]. ARPE19 cells produce more caspases through apoptosis when miMDys levels rise[39]. Given the increase in caspases and apoptosis, we expected that the miMDys, cOFR, LPO, and mOFR levels would rise as well.

The images of red (MitoTr), orange (JC1), BF (black/white), merge, and 2.5D were recorded using the CCD camera (Figure 4A), whereas the images of red (MitoSOX), green (DCF), merge, and 2.5D were recorded using the LSCM/800 (Figure 5A). The HPO showed greater concentrations of miMDys (JC1; Figure 4B), mOFR (MitoSOX; Figure 5B), cOFR (DCF; Figure 5C), and LPO (Table 1) than the CNT and RSV ($P<0.05$). However, after receiving RSV treatments, their levels were lowered ($P<0.05$) in the HPO+RSV.

An increase in these molecules was associated with a rise in miMDys after HPO incubation, even though RSV incubation decreased miMDys, which in turn decreased LPO, mOFR, and cOFR. Thus, the effects of RSV and HPO on the oxidative degeneration caused by TRPA1 activation in ARPE19 were further validated by the results of LPO, cOFR, mOFR, and miMDys.

RSV Attenuated HPO-Caused Decreases in GPx Activity and GSH Concentration *via* $[Zn^{2+}]_i$ Decreases in the Cells Thiol group members (GPx and GSH) are strong antioxidants, and effective scavengers of mOFR, LPO, and cOFR, in ARPE19[39,41]. Increases in mOFR, LPO, and cOFR are caused by the accumulation of Zn^{2+} in the mitochondria[39-40]. GSH was depleted in glioblastoma cells as a result of TRPA1 activation[42]. We suspected that the HPO-treated ARPE19 cells were inducing more $[Zn^{2+}]_i$ but less GPx and GSH after observing that they had greater amounts of LPO, mOFR, and cOFR. According to the green $[Zn^{2+}]_i$ (FluoZin3; Figure 6A) and

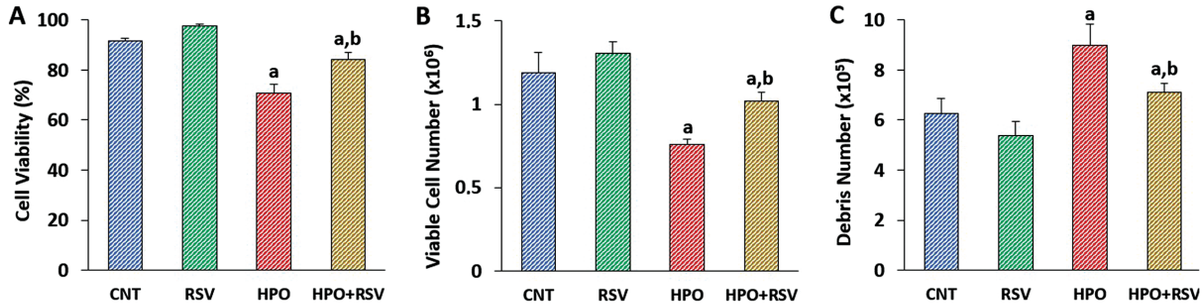

Figure 1 Changes in cell viability, number of viable cells, and debris caused by hypoxia (HPO) were modulated by resveratrol (RSV) The cell viability percentage (A), the number of viable cell (B), and the number of debris (C) were detected in the groups of control (CNT), RSV (50 μmol/L for 24h), HPO (200 μmol/L $CoCl_2$ for 24h), and HPO+RSV ([a]P<0.05 *vs* CNT and RSV; [b]P<0.05 *vs* HPO). Data are presented as mean±standard deviation, n=3. $CoCl_2$: Cobalt chloride.

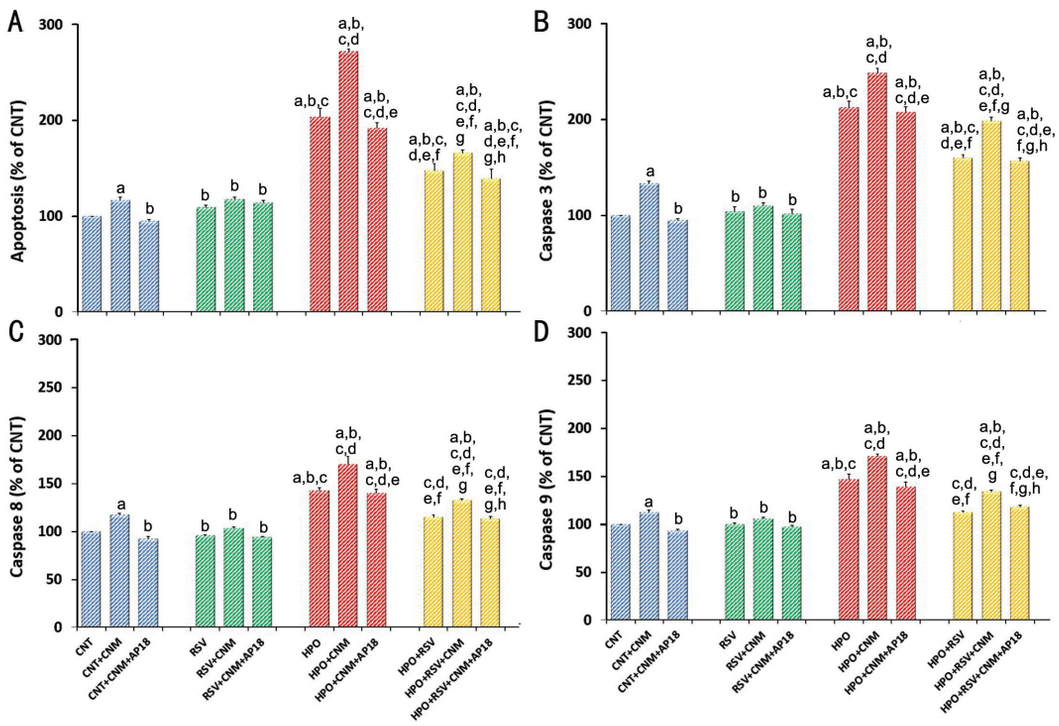

Figure 2 Treatments with RSV prevented HPO-induced increases in caspases and apoptosis through the inhibition of TRPA1 in ARPE19 In the CNT, RSV (50 μmol/L for 24h), HPO (200 μmol/L $CoCl_2$ for 24h), and their combinations (HPO+RSV), the percentages of apoptosis (A), caspase 3 (B), caspase 8 (C), and caspase 9 (D) were carried out. The analysis was repeated on cells in the four groups after 30min TRPA1 activation (0.1 mmol/L CNM) and 30min inhibition (20 μmol/L AP18). [a]P<0.05 *vs* CNT; [b]P<0.05 *vs* CNT+CNM; [c]P<0.05 *vs* RSV, RSV+CNM, and RSV+CNM+AP18; [d]P<0.05 *vs* HPO; [e]P<0.05 *vs* HPO+CNM; [f]P<0.05 *vs* HPO+CNM+AP18; [g]P<0.05 *vs* HPO+RSV; [h]P<0.05 *vs* HPO+RSV+CNM. Data are presented as mean±standard deviation, n=3. RSV: Resveratrol; HPO: Hypoxia; CNT: Control; $CoCl_2$: Cobalt chloride; TRPA1: Transient receptor potential ankyrin 1; CNM: Cinnamaldehyde; AP18: TRPA1 antagonist; ARPE19: Human retinal pigment epithelial cell 19.

GSH (ThiolTracker; Figure 6C) photos, the HPO exhibited a greater concentrations of $[Zn^{2+}]_i$ than the CNT and RSV, but a lower (P<0.05) GSH fluorescence concentration (Figure 6D), GPx activity and GSH levels (Table 1). The green images of HPO+RSV and HPO+AP18 indicated lower $[Zn^{2+}]_i$ (Figure 6B) but higher GSH levels than the HPO alone (Figure 6D). Based on current GSH and GPx data, TRPA1 activation is responsible for the HPO-induced reduction in GSH and GPx. The GSH and GPx reductions induced by HPO were prevented by the RSV and TRPA1 inhibitor (AP18) treatments.

HPO Increased $[Ca^{2+}]_i$ Concentration Though the TRPA1 Stimulation The HPO showed greater changes in $[Ca^{2+}]_i$ amount in the green (Fluo-3 AM) images (Figure 7A) in comparison to the CNT and RSV (P<0.05). The HPO+CNM had a higher $[Ca^{2+}]_i$ concentration than in the CNT+CNM (P<0.05), while the TRPA1 agonist (CNM) in the CNT and HPO induced the greatest amount of $[Ca^{2+}]_i$ in the cells (Figure 7B). The fluorescence intensity of $[Ca^{2+}]_i$ was diminished in the CNT+AP18 and HPO+AP18 groups as compared to CNT and HPO (P<0.05). When comparing the HPO+RSV

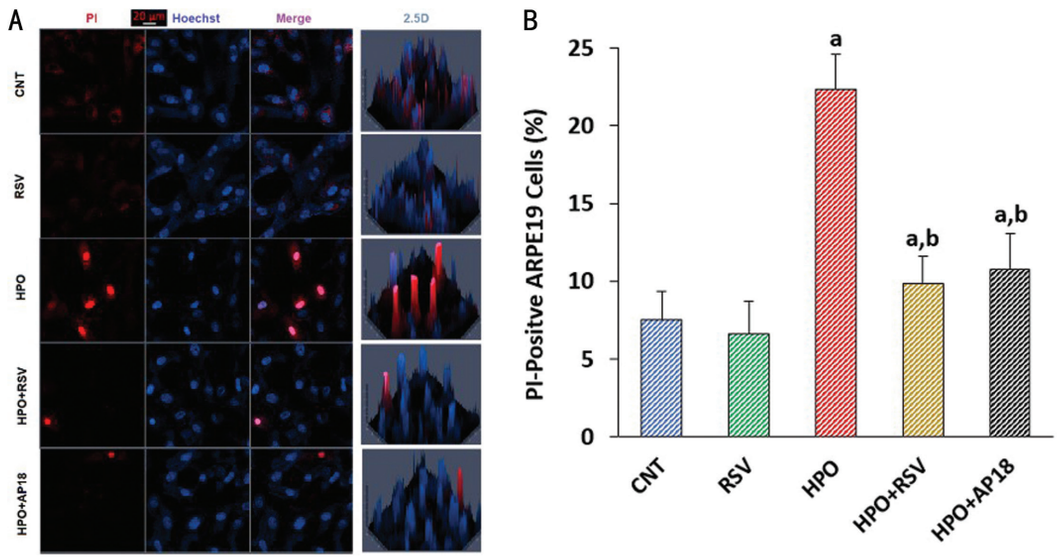

Figure 3 The count of death PI-positive ARPE19 cells was increased by the HPO (200 μmol/L $CoCl_2$ for 24h) while it was decreased by the RSV (50 μmol/L for 24h) A: Red (PI), blue (Hoechst), merge, and 2.5D images were taken using an LSM800 laser scan confocal microscope with a 20 (0.8)× objective. Scale bar: 20 μm. B: The percentages of PI-positive cells. [a]*P*<0.05 *vs* CNT and RSV; [b]*P*<0.05 *vs* HPO. Data are presented as mean±standard deviation, *n*=8. PI: Propidium iodide; ARPE19: Human retinal pigment epithelial cell 19; HPO: Hypoxia; $CoCl_2$: Cobalt chloride; RSV: Resveratrol; CNT: Control; AP18: TRPA1 antagonist.

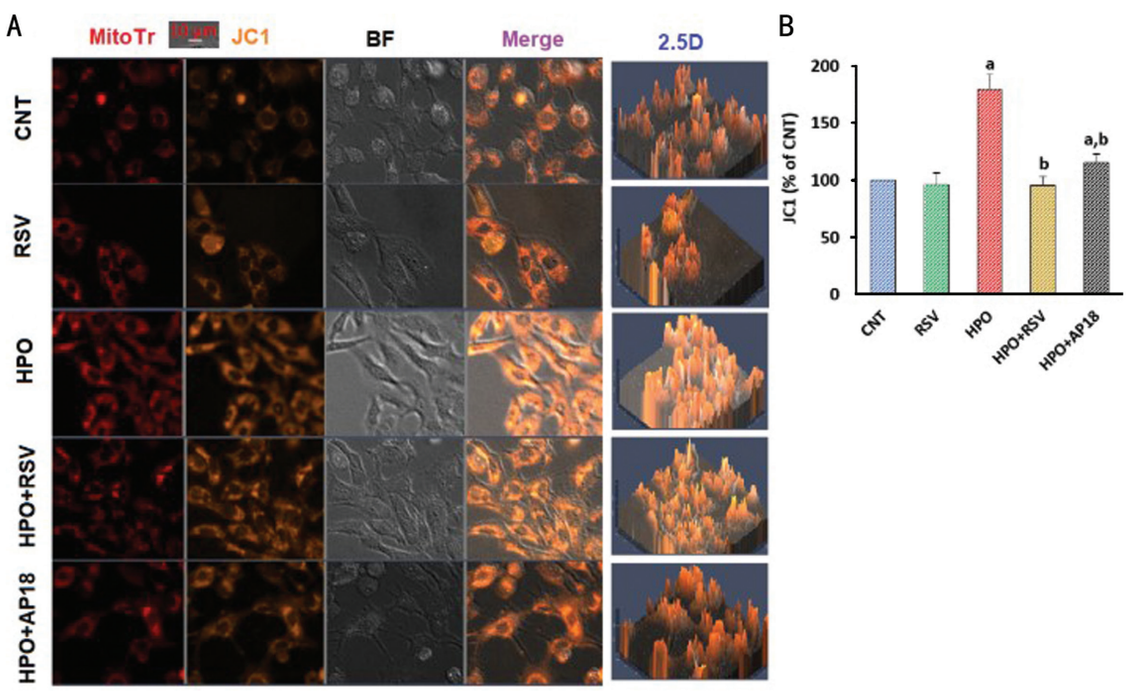

Figure 4 RSV (50 μmol/L for 24h) reduced HPO (200 μmol/L $CoCl_2$ for 24h)-induced increases in mitochondrial membrane dysfunction (miMDys) in ARPE19 A: A fluorescent CCD (Axiocam 702 microscopy) camera (Carl Zeiss) attached with a 20 (0.8)× objective was used to capture the images of red (MitoTracker), orange (JC1), BF (black/white), merge, and 2.5D. Scale bar: 10 μm. B: The percentages of miMDys (JC1). [a]*P*<0.05 *vs* CNT and RSV; [b]*P*<0.05 *vs* HPO. Data are presented as mean±standard deviation, *n*=8. RSV: Resveratrol; HPO: Hypoxia; $CoCl_2$: Cobalt chloride; ARPE19: Human retinal pigment epithelial cell 19; CCD: Charge-coupled device; BF: Bright field; CNT: Control; AP18: TRPA1 antagonist.

to the HPO alone, the effects were less noticeable (P<0.05). Responses from HPO+RSV and HPO+RSV+CNM were similar to the CNT values, and there were no changes in $[Ca^{2+}]_i$ concentrations in the cells after the CNM stimulation. Therefore, we observed that the TRPA1-mediated elevation of $[Ca^{2+}]_i$ was enhanced in ARPE19 by the HPO induction, although the elevations were diminished by the treatment of RSV and TRPA1 antagonist (AP18).

DISCUSSION

The development of aberrant neovascularization is largely influenced by retinal HPO. This makes it the primary cause of vision loss in neovascular retinal diseases[1-2]. $[Ca^{2+}]_i$ overload

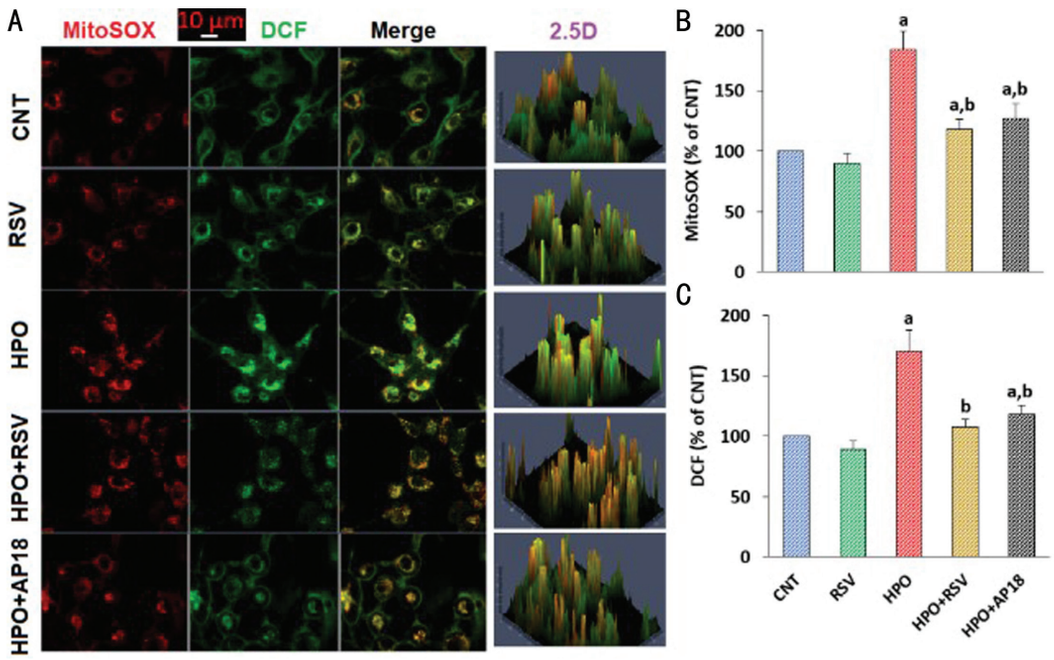

Figure 5 HPO (200 μmol/L $CoCl_2$ for 24h)-induced increases mOFR and cOFR were decreased in ARPE19 by the RSV (50 μmol/L for 24h) treatment A: The images of red MitoSOX (mOFR), green DCF (cOFR), merged, and 2.5D were taken in the LSM800 laser scanning confocal microscope attached with a 20× objective. Scale bar: 10 μm. B, C: The percentages of MitoSOX and DCF. [a]*P*<0.05 *vs* CNT and RSV; [b]*P*<0.05 *vs* HPO. Data are presented as mean±standard deviation, *n*=8. HPO: Hypoxia; $CoCl_2$: Cobalt chloride; mOFR: Mitochondrial oxygen free radical; cOFR: Cytosolic oxygen free radical; RSV: Resveratrol; ARPE19: Human retinal pigment epithelial cell 19; DCF: Dichlorofluorescein; CNT: Control; AP18: TRPA1 antagonist.

Table 1 RSV treatment enhanced the HPO-induced decreases in GSH levels and GPx activity through the reduction of LPO concentrations in ARPE19 cells

Parameters	CNT	RSV	HPO	HPO+RSV
GPx (IU/g protein)	20.90±0.83	21.80±1.83	15.60±0.69[a]	20.00±2.38[b]
GSH (μmol/L/g protein)	14.41±1.20	14.53±0.48	8.61±0.41[a]	12.43±0.83[a,b]
LPO (μmol/L/g protein)	20.18±1.82	18.65±1.99	29.43±1.94[a]	24.63±1.27[a,b]

[a]*P*<0.05 *vs* CNT and RSV; [b]*P*<0.05 *vs* HPO. RSV treatments (50 μmol/L for 24h) enhanced HPO (200 μmol/L $CoCl_2$ for 24h)-induced decreases in diminished GPx activity and GSH levels through the reduction of LPO concentrations in ARPE19 (mean±standard deviation and *n*=4). CNT: Control; RSV: Resveratrol; HPO: Hypoxia; $CoCl_2$: Cobalt chloride; GPx: Glutathione peroxidase; GSH: Reduced glutathione; LPO: Lipid peroxidation; ARPE19: Human retinal pigment epithelial cell 19.

is one of the processes by which HPO causes retinal oxidative stress, apoptosis and death[7]. Retinal death and apoptosis are caused by the permeability transition pores opening and the depolarization of the inner membrane of mitochondria as a result of an increase in $[Ca^{2+}]_i$[24]. Therefore, new techniques to prevent and reduce excessive accumulation of the $[Ca^{2+}]_i$ during HPO are desperately needed to cure retinal degeneration. RSV therapy produced a protective effect on oxidative degeneration and apoptosis in neurons *via* the regulation of the TRP channels such as TRPM2 and TRPV4[9,25-26]. There is no report on the protective action of RSV and TRPA1 on apoptosis and mitochondrial oxidative stress in the HPO of ARPE19 cells. We first investigated the involvement of TRPA1 in the hypoxic damage of ARPE19 cells using measurements of apoptosis, cell death, miMDy, and mOFR. Second, the modulator action of RSV on oxidative degeneration and apoptosis levels was investigated using TRPA1 inhibition.

Based on current data, we found that HPO increased oxidants (mOFR, cOFR, LPO, miMDys), cell death, debris number, apoptosis, and caspases (CASP/3, CASP/8, and CASP/9) through an increase in TRPA1 stimulation-mediated $[Ca^{2+}]_i$ and $[Zn^{2+}]_i$, but diminished cell viability percentage, viable cell number, GSH, and GPx in the ARPE19 cells. However, the RSV therapy lessened the alterations. Using the TRPA1 blocker (AP18), the role of TRPA1 in the oxidant, cell death, and apoptotic effects of HPO was further verified. However, the RSV treatments altered the oxidant and apoptotic actions of HPO *via* TRPA1 suppression in the ARPE19 cells.

The HPO-induced mOFR and cOFR oxidants directly gate the TRPA1 in retinal cells[15-16]. The apoptotic action of CNM

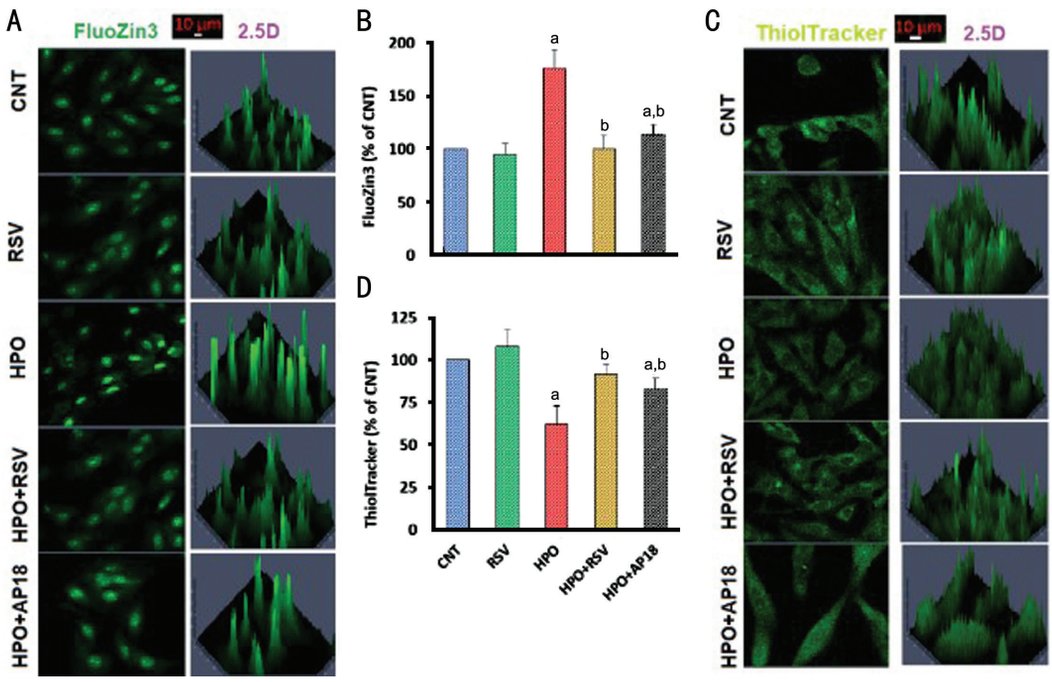

Figure 6 The intracellular free zinc ($[Zn^{2+}]_i$) concentration increases were reduced by RSV (50 μmol/L for 24h), while GSH decreases induced by HPO (200 μmol/L $CoCl_2$ for 24h) were increased The images of FluoZin3 AM ($[Zn^{2+}]_i$) (A) and ThiolTracker Violet (GSH) (C) were recorded in the LSM800 microscope. Scale bar: 10 μm. Objective: 20×. The FluoZin3 (B) and ThiolTracker (D) expressions were presented using the control percentage. [a]*P*<0.05 *vs* CNT and RSV; [b]*P*<0.05 *vs* HPO. Data are presented as mean±standard deviation, *n*=8. RSV: Resveratrol; GSH: Glutathione; HPO: Hypoxia; $CoCl_2$: Cobalt chloride; CNT: Control; AP18: TRPA1 antagonist.

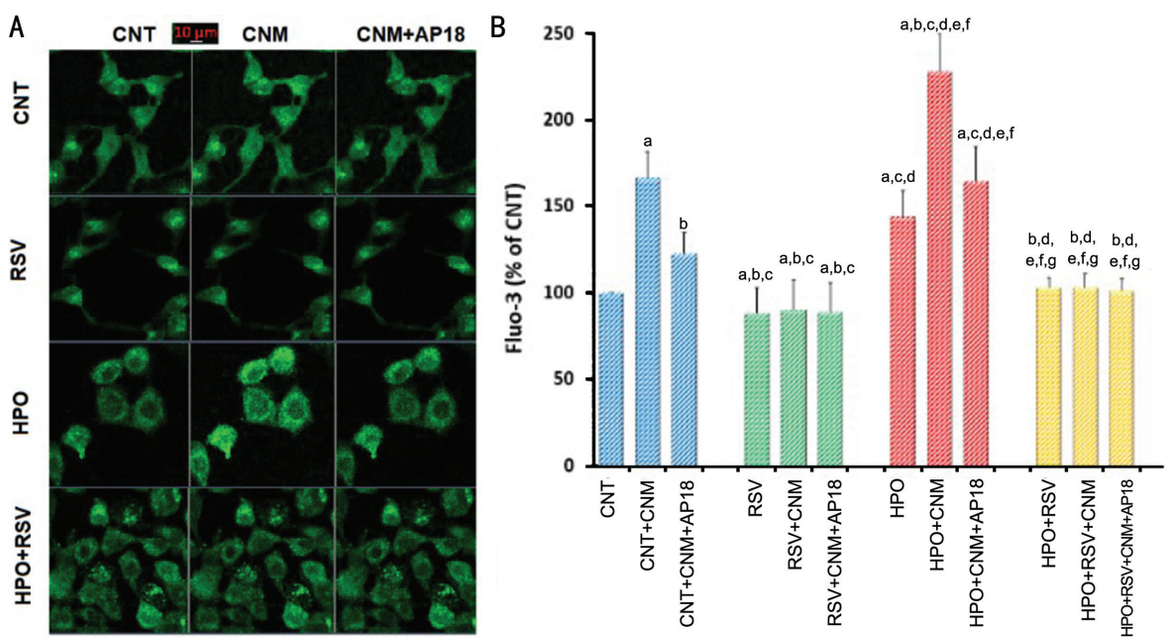

Figure 7 Resveratrol (RSV) diminished the increase in $[Ca^{2+}]_i$ in ARPE19 caused by hypoxia (HPO) TRPA1 channel in the stained (Fluo-3 AM) cells were stimulated with CNM (0.1 mmol/L) for 60–90s and subsequently inhibited in the LSM800 microscope with 20 μmol/L AP18 for 60–90s. A: The representative images of Fluo-3 AM of Control (CNT), RSV (50 μmol/L for 24h), HPO (200 μmol/L $CoCl_2$ for 24h), and HPO+RSV. B: Following the RSV and CNM incubations, the mean fluorescence intensity changes of four groups as a percentage of control. Scale bar: 10 μm. [a]*P*<0.05 *vs* CNT; [b]*P*<0.05 *vs* CNT+CNM; [c]*P*<0.05 *vs* CNT+CNM+AP18; [d]*P*<0.05 *vs* RSV, RSV+CNM, and RSV+CNM+AP18; [e]*P*<0.05 *vs* HPO; [f]*P*<0.05 *vs* HPO+CNM; [g]*P*<0.05 *vs* HPO+CNM+RSV). Data are presented as mean±standard deviation, *n*=6. ARPE19: Human retinal pigment epithelial cell 19; CNM: Cinnamaldehyde; AP18: TRPA1 antagonist.

treatment in hypoxic colorectal cancer cells was reported[43]. Gating TRPA1 *via* CNM and OFRs induced an increase in $[Ca^{2+}]_i$ in the rat hippocampus[33] and glioblastoma cells[19,32], although its inhibition *via* AP18 decreased the $[Ca^{2+}]_i$

concentration in the cells. Consistent with the data, the HPO induction-mediated increase in $[Ca^{2+}]_i$ in the ARPE19 cells was further augmented through TRPA1 stimulation. However, the Ca^{2+} influxes were reduced in the cells by the TRPA1 blocker (AP18), indicating the involvement of TRPA1 in HPO-caused Ca^{2+} influx. Accumulating data indicate that natural components such as RSV and piperine play a major protective role in HPO-induced retinal injury[21,23,44]. Involvements of TRPM2 and TRPV4 in HPO-induced oxidative injury and $[Ca^{2+}]_i$ accumulation in the neuronal cells were recently reported[25-26]. A modulatory role of RSV on HPO-caused increases in $[Ca^{2+}]_i$ concentration in the rat H9c2 heart cells was reported more recently[45]. In the current results, we found that RSV modulates the activation of TRPA1 in the ARPE19 cells caused by HPO. Therefore, the TRPA1 and RSV findings in the neural cells were validated by the data[9,25-26,33].

Mitochondria act major functions in the generation of OFRs. A growing number of studies suggest that the buildup of Ca^{2+} and Zn^{2+} in mitochondria causes an excess of OFRs to be generated, raising miMDys[11,42]. By upregulating TRPA1 activation and miMDys levels in the tumor cells, HPO caused excessive cOFR and mOFR generation[19,46]. However, RSV treatment prevented these aberrant processes in the heart cells and cardiomyocytes[45,47]. The current evidence indicates that HPO induced the miMDys, cOFR, and mOFR processes in the ARPE19 cells. However, the RSV treatment reduced the cOFR, mOFR, and miMDys processes in the ARPE19 cells by inhibiting TRPA1. It appears that increased OFR production is caused by an increase in miMDys through an increase in TRPA1-dependent Ca^{2+} and Zn^{2+} influx into mitochondria. TRPA1 activation, mOFR, and miMDys generation were accelerated as a result of the process being expedited during HPO, which also increased cOFR, LPO, and mOFR generation. This, in turn, increased OFR generation, which in turn produced a cycle of ARPE19 death. We believe that the TRPA1 modulating property of RSV blocks these aberrant activities.

ARPE19 cell death is intimately linked to HPO, and the synthesis of OFR is a key factor in apoptosis of these cells *via* $[Ca^{2+}]_i$ overload[22]. We found that exposing ARPE19 cells to HPO reduced cell viability percentage and number by suppressing the GPx activity and GSH levels. These results are consistent with these observations[7,22]. The generations of cOFR and mOFR may result from a pro- and anti-oxidant redox system imbalance. After HPO induction, it was found that the levels of cOFR in the Müller cell diabetes model rose due to the overexpression of TRPV4 channels and apoptosis, along with the downregulation of GSH and GPx[48].

We demonstrated in HPO-induced ARPE19 cells that RSV reduced the production of mOFR, cOFR, and LPO while increasing GPx and GSH levels. By inhibiting the TRPA1

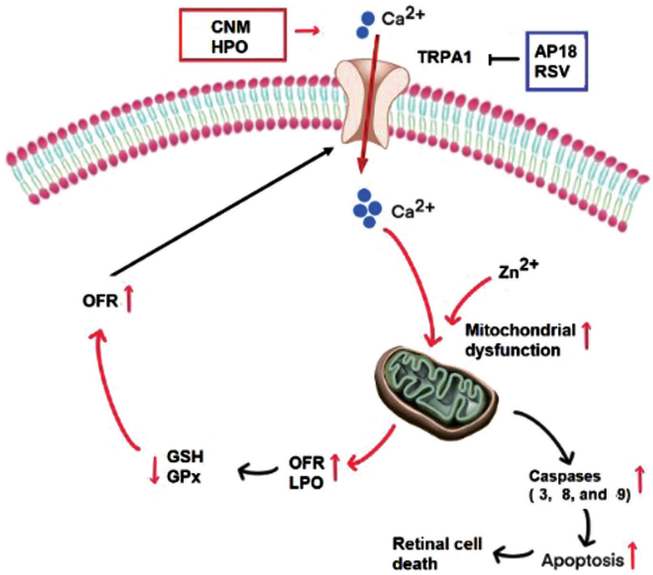

Figure 8 Hypoxia (HPO) may influence oxidative degeneration and apoptosis in human retinal pigment epithelial cells (ARPE19) by stimulating transient receptor potential ankyrin 1 (TRPA1) channel

Ca^{2+} concentration in the ARPE19 increases when TRPA1 is stimulated by HPO (cinnamaldehyde, CNM). Two mechanisms are triggered by Ca^{2+} accumulation in the mitochondria: 1) stimulation of active caspase 3, 8, and 9, which causes apoptosis and retinal cell death; 2) a decrease in glutathione (GSH) concentration and glutathione peroxidase (GPx) activity but an increase in and lipid peroxidation (LPO) and oxygen free radicals (OFR). Treatment with resveratrol (RSV) causes TRPA1 inhibition to reverse the HPO-mediated pathways. AP18: TRPA1 antagonist.

and TRPM2[11,19], RSV reversed early apoptosis and the loss of mitochondrial depolarization caused by HPO, which was a hallmark of OFRs-mediated miMDys[19]. Although RSV incubation moderated the alterations, the TRPA1 agonist (HC-030031) increased apoptosis and Ca^{2+} overload in human prostate cancer cells[49]. HPO and TRPA1 agonist (CNM) downregulated cell viability and viable cell quantity, which led to an increase in cell death (PI positive cell percentage) and the primary apoptosis triggers and regulators (CASP/3, CASP/8, and CASP/9)[21], whereas RSV and TRPA1 antagonist (AP18) reversed the increases. These results suggest that RSV has strong TRPA1 inhibitory effects against HPO-induced oxidative damage and ARPE19 cell death (Figure 8).

GSH and GPx are important components of the thiol redox system[48]. TRPA1 has high content of cysteine residues in its structure, making it the most vulnerable subgroup of the TRP superfamily to excessive mOFR and cOFR synthesis[15]. Therefore, cOFR and mOFR modify cysteine-free sulfhydryl groups to activate TRPA1[50]. In this study, when HPO stimulated the TRPA1 channel, GSH and GPx levels decreased. However, GSH levels and GPx activity increased when RSV therapy blocked the channel.

In conclusion, our findings show that TRPA1 inhibition successfully reduced the HPO-caused oxidative degeneration and cell death responses in ARPE19 cells. Furthermore, the RSV treatment prevented the HPO-induced elevations in apoptotic mediators (CASP/3, CASP/8, and CASP/9), Zn^{2+} influx, Ca^{2+} overload, oxidants (LPO, miMDys, cOFR, and mOFR), and cell death by lowering TRPA1 activity in the cells. This was the first study to suggest that RSV treatment might improve defenses against oxidative stress and ARPE19 cell death caused by HPO, perhaps by blocking TRPA1 activity. The present investigation offers a novel therapeutic approach for preventing HPO-induced retinal oxidative damage by inhibiting TRPA1 activity.

ACKNOWLEDGEMENTS

Authors' Contributions: Each author made a contribution to the definition, design, and conceptualization of the study's intellectual content. Argun M: Analyzed/interpreted data, provided material, and financial application, and proofed/revised the article. Nazıroğlu M: Designed the experiment, conducted the experiment, analyzed/interpreted data, and wrote the article.

Data Availability Statement: The information is available upon request from Naziroğlu M.

AI-Generated Content Disclosure: None.

Foundations: Supported by BSN Health, Analyses, Innovation, Consultancy, Organization, Agriculture, Industry LTD, Isparta, Türkiye (No.2023-10).

Conflicts of Interest: Argun M, None; **Nazıroğlu M,** None.

REFERENCES

1 Shinojima A, Lee D, Tsubota K, *et al*. Retinal diseases regulated by hypoxia—basic and clinical perspectives: a comprehensive review. *J Clin Med* 2021;10(23):5496.

2 Srejovic JV, Muric MD, Jakovljevic VL, *et al*. Molecular and cellular mechanisms involved in the pathophysiology of retinal vascular disease-interplay between inflammation and oxidative stress. *Int J Mol Sci* 2024;25(21):11850.

3 Lee CY, Yang CH. The role of fractalkine in diabetic retinopathy: pathophysiology and clinical implications. *Int J Mol Sci* 2025;26(1):378.

4 Huang KC, Chiang YF, Ali M, *et al*. Oleocanthal mitigates $CoCl_2$-induced oxidative damage and apoptosis *via* regulating MAPK pathway in human retinal pigment epithelial cells. *Biomed Pharmacother* 2024;180:117582.

5 Xue R, Fan XL, Yang Q, *et al*. Protective effect of ethyl ferulate against hypoxic injury in retinal cells and retinal neovascularization in an oxygen-induced retinopathy model. *Phytomedicine* 2023;121:155097.

6 Ahmad A, Nawaz MI, Siddiquei MM, *et al*. Apocynin ameliorates NADPH oxidase 4 (NOX4) induced oxidative damage in the hypoxic human retinal Müller cells and diabetic rat retina. *Mol Cell Biochem* 2021;476(5):2099-2109.

7 Özkaya D, Naziroğlu M, Vanyorek L, *et al*. Involvement of TRPM2 channel on hypoxia-induced oxidative injury, inflammation, and cell death in retinal pigment epithelial cells: modulator action of selenium nanoparticles. *Biol Trace Elem Res* 2021;199(4):1356-1369.

8 Öcal Ö, Coşar A, Naziroğlu M. Amantadine attenuated hypoxia-induced mitochondrial oxidative neurotoxicity, apoptosis, and inflammation *via* the inhibition of TRPM2 and TRPV4 channels. *Mol Neurobiol* 2022;59(6):3703-3720.

9 Özşimşek A, Naziroğlu M. The involvement of TRPV4 on the hypoxia-induced oxidative neurotoxicity and apoptosis in a neuronal cell line: Protective role of melatonin. *Neurotoxicology* 2021;87:136-148.

10 Liu PP, Chen J, Qi JY, *et al*. Hesperetin ameliorates ischemia/hypoxia-induced myocardium injury *via* inhibition of oxidative stress, apoptosis, and regulation of Ca^{2+} homeostasis. *Phytother Res* 2023;37(5):1787-1805.

11 Ravi R, Subramaniam Rajesh B. Paraoxonase 2 protects against the CML mediated mitochondrial dysfunction through modulating JNK pathway in human retinal cells. *Biochim Biophys Acta Gen Subj* 2022;1866(1):130043.

12 Tong Y, Wang SS. Not all stressors are equal: mechanism of stressors on RPE cell degeneration. *Front Cell Dev Biol* 2020;8:591067.

13 Namer B, Seifert F, Handwerker HO, *et al*. TRPA1 and TRPM8 activation in humans: effects of cinnamaldehyde and menthol. *Neuroreport* 2005;16(9):955-959.

14 Petrus M, Peier AM, Bandell M, *et al*. A role of TRPA1 in mechanical hyperalgesia is revealed by pharmacological inhibition. *Mol Pain* 2007;3:40.

15 Sakaguchi R, Mori Y. Transient receptor potential (TRP) channels: Biosensors for redox environmental stimuli and cellular status. *Free Radic Biol Med* 2020;146:36-44.

16 Souza Monteiro de Araújo D, De Logu F, Adembri C, *et al*. TRPA1 mediates damage of the retina induced by ischemia and reperfusion in mice. *Cell Death Dis* 2020;11(8):633.

17 Alizadehasl A, Alavi MS, Alavi MS, *et al*. TRPA1 as a promising target in ischemia/reperfusion: a comprehensive review. *Iran J Basic Med Sci* 2024;27(3):270-278.

18 Pires PW, Earley S. Neuroprotective effects of TRPA1 channels in the cerebral endothelium following ischemic stroke. *eLife* 2018;7:e35316.

19 Deveci HA, Akyuva Y, Nur G, *et al*. Alpha lipoic acid attenuates hypoxia-induced apoptosis, inflammation and mitochondrial oxidative stress *via* inhibition of TRPA1 channel in human glioblastoma cell line. *Biomed Pharmacother* 2019;111:292-304.

20 Qin SY, Cao GP, Tang MX, *et al*. Baicalin alleviates the injury of human retinal pigment epithelium cells and improves branch retinal vein occlusion in rats by inhibiting the HIF-1α/VEGFA axis. *Eur J Med Res* 2024;29(1):564.

21 Golmohammadi M, Meibodi SAA, Al-Hawary SIS, *et al*. Neuroprotective effects of resveratrol on retinal ganglion cells in glaucoma in rodents: a narrative review. *Animal Model Exp Med* 2024;7(3):195-207.

22 Roumes H, Goudeneche P, Pellerin L, *et al*. Resveratrol and some of its derivatives as promising prophylactic treatments for neonatal hypoxia-ischemia. *Nutrients* 2022;14(18):3793.

23 Xin XR, Dang H, Zhao XJ, *et al*. Effects of hypobaric hypoxia on rat retina and protective response of resveratrol to the stress. *Int J Med Sci* 2017;14(10):943-950.

24 Daldal H, Naziroğlu M. Selenium and resveratrol attenuated diabetes mellitus-mediated oxidative retinopathy and apoptosis *via* the modulation of TRPM2 activity in mice. *Biol Trace Elem Res* 2022;200(5):2283-2297.

25 Osmanlioğlu HÖ, Naziroğlu M. Resveratrol modulates diabetes-induced neuropathic pain, apoptosis, and oxidative neurotoxicity in mice through TRPV4 channel inhibition. *Mol Neurobiol* 2024;61(9):7269-7286.

26 Akyuva Y, Naziroğlu M. Resveratrol attenuates hypoxia-induced neuronal cell death, inflammation and mitochondrial oxidative stress by modulation of TRPM2 channel. *Sci Rep* 2020;10(1):6449.

27 Matsumoto Y, Komatsu K, Shimazu Y, *et al*. Effect of resveratrol on *c-fos* expression of rat trigeminal spinal nucleus caudalis and C1 dorsal horn neurons following mustard oil-induced acute inflammation. *Eur J Oral Sci* 2017;125(5):338-344.

28 Mergler S, Derckx R, Reinach PS, *et al*. Calcium regulation by temperature-sensitive transient receptor potential channels in human uveal melanoma cells. *Cell Signal* 2014;26(1):56-69.

29 Maugeri A, Barchitta M, Mazzone MG, *et al*. Resveratrol modulates SIRT1 and DNMT functions and restores LINE-1 methylation levels in ARPE-19 cells under oxidative stress and inflammation. *Int J Mol Sci* 2018;19(7):2118.

30 Josifovska N, Albert R, Nagymihály R, *et al*. Resveratrol as inducer of autophagy, pro-survival, and anti-inflammatory stimuli in cultured human RPE cells. *Int J Mol Sci* 2020;21(3):813.

31 Cheng BC, Chen JT, Yang ST, *et al*. Cobalt chloride treatment induces autophagic apoptosis in human glioma cells *via* a p53-dependent pathway. *Int J Oncol* 2017;50(3):964-974.

32 Ovey IS, Ozsimsek A, Velioglu HA, *et al*. EGb 761 reduces Ca^{2+} influx and apoptosis after pentylenetetrazole treatment in a neuroblastoma cell line. *Front Cell Neurosci* 2023;17:1195303.

33 Övey IS, Naziroğlu M. Effects of homocysteine and memantine on oxidative stress related TRP cation channels in *in-vitro* model of Alzheimer's disease. *J Recept Signal Transduct Res* 2021;41(3):273-283.

34 Ertilav K. Pregabalin protected cisplatin-induced oxidative neurotoxicity in neuronal cell line. *J Cell Neurosci Oxid Stress* 2019;11(1):815-824.

35 Uğuz AC, Naziroğlu M, Espino J, *et al*. Selenium modulates oxidative stress-induced cell apoptosis in human myeloid HL-60 cells through regulation of calcium release and caspase-3 and-9 activities. *J Membr Biol* 2009;232(1):15-23.

36 Placer ZA, Cushman LL, Johnson BC. Estimation of product of lipid peroxidation (malonyl dialdehyde) in biochemical systems. *Anal Biochem* 1966;16(2):359-364.

37 Sedlak J, Lindsay RH. Estimation of total, protein-bound, and nonprotein sulfhydryl groups in tissue with Ellman's reagent. *Anal Biochem* 1968;25(1):192-205.

38 Lawrence RA, Burk RF. Glutathione peroxidase activity in selenium-deficient rat liver. *Biochem Biophys Res Commun* 1976;71(4):952-958.

39 Ertuğrul A, Özkaya D, Naziroğlu M. Curcumin attenuates hydroxychloroquine-mediated apoptosis and oxidative stress *via* the inhibition of TRPM2 channel signalling pathways in a retinal pigment epithelium cell line. *Graefes Arch Clin Exp Ophthalmol* 2023;261(10):2829-2844.

40 AlAhmad M, Isbea H, Shitaw E, *et al*. NOX2-TRPM2 coupling promotes Zn^{2+} inhibition of complex III to exacerbate ROS production in a cellular model of Parkinson's disease. *Sci Rep* 2024;14(1):18431.

41 Yang YC, Liu MT, Dong X, *et al*. Naringin suppresses $CoCl_2$-induced ferroptosis in ARPE-19 cells. *Antioxidants* (*Basel*) 2025;14(2):236.

42 Chen H, Li CL, Hu HY, *et al*. Activated TRPA1 plays a therapeutic role in TMZ resistance in glioblastoma by altering mitochondrial dynamics. *BMC Mol Cell Biol* 2022;23(1):38.

43 Wu CE, Zhuang YW, Zhou JY, *et al*. Cinnamaldehyde enhances apoptotic effect of oxaliplatin and reverses epithelial-mesenchymal transition and stemness in hypoxic colorectal cancer cells. *Exp Cell Res* 2019;383(1):111500.

44 Zhang P, Zhou YD, Tan Y, *et al*. Protective effects of piperine on the retina of mice with streptozotocin-induced diabetes by suppressing HIF-1/VEGFA pathway and promoting PEDF expression. *Int J Ophthalmol* 2021;14(5):656-665.

45 Wu X, Zhou SS, Zhu N, *et al*. Resveratrol attenuates hypoxia/reoxygenation-induced Ca^{2+} overload by inhibiting the Wnt5a/Frizzled-2 pathway in rat H9c2 cells. *Mol Med Rep* 2014;10(5):2542-2548.

46 Du H, Zhang L, Feng JJ, *et al*. Enhancing photodynamic therapy efficacy *via* photo-triggered calcium overload and oxygen delivery in tumor hypoxia management. *ACS Appl Mater Interfaces* 2025;17(5):8403-8416.

47 Li T, Chen LL, Yu YY, *et al*. Resveratrol alleviates hypoxia/reoxygenation injury-induced mitochondrial oxidative stress in cardiomyocytes. *Mol Med Rep* 2019;19(4):2774-2780.

48 Chen Z, Liu BJ, Zhou DJ, *et al*. AQP4 regulates ferroptosis and oxidative stress of Muller cells in diabetic retinopathy by regulating TRPV4. *Exp Cell Res* 2024;439(1):114087.

49 Vancauwenberghe E, Noyer L, Derouiche S, *et al*. Activation of mutated TRPA1 ion channel by resveratrol in human prostate cancer associated fibroblasts (CAF). *Mol Carcinog* 2017;56(8):1851-1867.

50 Hinman A, Chuang HH, Bautista DM, *et al*. TRP channel activation by reversible covalent modification. *Proc Natl Acad Sci U S A* 2006;103(51):19564-19568.